

Experimental Determination of Electron Deformation Density Distribution in a Cu(II) Complex of α -Aminooxyacetic Acid

Jorunn Sletten^{a,b,*} and Håkon Hope^b

^aDepartment of Chemistry, University of Bergen, Allégate 41, N-5007 Bergen, Norway and ^bDepartment of Chemistry, University of California, Davis, California 95616, USA

Sletten, J. and Hope, H., 1988. Experimental Determination of Electron Deformation Density Distribution in a Cu(II) Complex of α -Aminooxyacetic Acid. – Acta Chem. Scand., Ser. A 42: 61–70.

The structure of bis(α -aminooxyacetato)copper(II) tetrahydrate, $[\text{Cu}(\text{C}_2\text{H}_4\text{NO}_3)_2(\text{H}_2\text{O})_2] \cdot 2\text{H}_2\text{O}$, has been refined using X-ray data collected at 85 K. The space group is *Pbca* with $a = 5.1612(5)$, $b = 18.760(2)$, $c = 10.972(1)$ Å, $Z = 4$ and $\mu(\text{MoK}\alpha) = 2.109 \text{ mm}^{-1}$. Full-matrix least-squares refinements based on all data ($0.0 < \sin\theta/\lambda < 1.39 \text{ \AA}^{-1}$) and with high-angle data (various $\sin\theta/\lambda$ limits) were performed, and the results are compared. Refinement with all data gave $R = 0.0222$, $S = 1.90$, and with high-angle data ($0.80 < \sin\theta/\lambda < 1.25 \text{ \AA}^{-1}$) $R = 0.0186$, $S = 1.08$. Electron deformation density maps have been calculated using the structure model obtained from high-angle refinements. The dominant features in the deformation density close to Cu are holes on the four short Cu-X bonds (X = O1, N), peaks in directions avoiding ligands, and lower positive regions on the two long Cu-O4 bonds. This is qualitatively consistent with crystal-field theory for Cu^{2+} in a Jahn-Teller distorted octahedral environment. Lone-pair and bond peaks in the ligands conform reasonably well with previous findings for light-atom structures. Inclusion of the highest angle data ($\sin\theta/\lambda > 1.25 \text{ \AA}^{-1}$) in the refinement causes more pronounced asymmetry in the deformation density around Cu, while features in the ligands are essentially unchanged.

Dedicated to Professor Olav Foss on his 70th birthday

Spatial distributions of *d*-electrons in transition metal ions have been studied in a number of cases using X-ray diffraction methods. Only a small number of copper(II) compounds have been studied,^{1–5} and, to our knowledge, these have all been complexes with inorganic ligands. The present compound (Fig. 1), which is a centrosymmetric Cu(II) complex with two small organic bidentate ligands in the equatorial plane and two axially coordinated water molecules, appeared well suited for an extension of the data on Cu(II). From a previous room temperature, low-angle investigation⁶ it was known that large crystals are easy to grow, and could possibly be shaped into spheres to minimize the problem of absorption correction. Since the scattering of the *d*-electrons of the heavier elements in the first transition se-

ries extends far out in reciprocal space,¹ it was considered important to collect data as far out in 2θ as the geometry of the instrument would permit. Also in this respect the present compound seemed advantageous on the basis of observations made for room temperature data collection.

Experimental

The compound was synthesized according to the procedure described by Zvilichovsky,⁷ and was recrystallized from water by slow evaporation at room temperature. Crystals were cut approximately to cubes and subsequently ground to spheres by tumbling in an abrasive-lined cylinder. A suitable abrasive and speed of air stream were found after several trial runs.

X-Ray data collection. Crystal data and experimental conditions are summarized in Table 1. A

*To whom correspondence should be addressed.

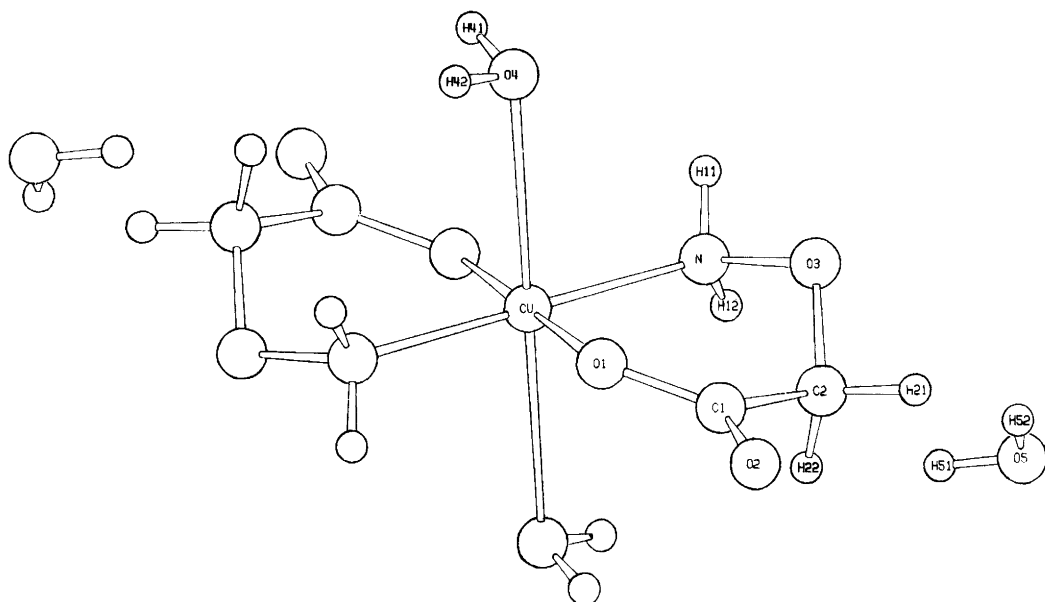


Fig. 1. Complex unit of the compound studied. Cu is situated at an inversion center.

sphere of diameter 0.46(1) mm was mounted on a Picker card-controlled diffractometer equipped with an Enraf-Nonius gas-flow cooling device modified for improved stability and lower temperature. For all measurements, graphite-monochromated MoK α radiation and a scintillation detector with a pulse-height analyzer were used. Cell dimensions at 85 K were determined by least-squares fitting to the diffractometer set-

tings for 14 reflections with 2θ in the region 92–116°, where α_1 and α_2 peaks are clearly separated ($\lambda_1 = 0.70926$ Å). All reflections within one octant were collected up to $2\theta = 70^\circ$. For 2θ between 70 and 163° only reflections predicted on the basis of parameters from a low-angle, low-temperature data set to have $I > 6\sigma_I$ were measured. This procedure has proven useful for a number of light-atom structures, and was

Table 1. Crystal data and experimental conditions.

Molecular formula	[Cu(C ₂ H ₄ NO ₃) ₂ (H ₂ O) ₂].2H ₂ O
Formula weight	315.72
Space group	<i>Pbca</i>
Unit cell at 85 K/Å, Å ³	<i>a</i> = 5.1612(5), <i>b</i> = 18.760(2) <i>c</i> = 10.971(1), <i>V</i> = 1062.3(4)
<i>D_x</i> /kg m ⁻³	1973
Radiation (λ /Å)	MoK α ($\lambda_1 = 0.70926$, $\lambda_2 = 0.71354$)
Monochromator	Graphite
Scan mode; speed in 2θ /°min ⁻¹	$\theta/2\theta$; 2
Scan range/°	[$2\theta(\alpha_1) - 1.1$] to [$2\theta(\alpha_2) + 1.1$]
($\sin\theta/\lambda$) _{max} /Å ⁻¹	1.386
No. of unique refl. measured	5314
μ (MoK α)/mm ⁻¹	2.109
Crystal size/mm	Sphere, <i>r</i> = 0.23
Transmission factors	0.478–0.524

adopted to avoid spending time measuring a large number of barely detectable reflections.⁸⁻¹⁰ A total of 5314 independent reflections were recorded using the $\theta/2\theta$ scan mode with scan speed $2^\circ (2\theta) \text{ min}^{-1}$ and scan ranges $[2\theta(\alpha_1)-1.1^\circ]$ to $[2\theta(\alpha_2)+1.1^\circ]$. Background intensities were measured for 20 s at each end of the scans. Attenuator filters kept the count rate below $10\,000 \text{ s}^{-1}$ to minimize coincidence losses. To check the agreement between symmetry equivalent intensities, 100 reflections from different regions of reciprocal space were measured in the hkl and $hk\bar{l}$ octants. Throughout the data collection four standards were measured every 100 reflections. Two standards of medium intensity (1,15,5 and 104) showed a 1–3% decrease in intensity over the data collection period, reflecting slight radiation damage. The other two (020 and 084) are very strong, and showed 10 and 4% increases in intensity, respectively, during the same period, indicating a time-variable extinction effect. After completion of the main data collection, the crystal was therefore brought to room temperature and exposed continuously to the X-ray beam until no further change was observed in the intensity of 020, the most intense reflection in the data set. After cooling to 85 K again all independent reflections in the range $0^\circ < 2\theta < 36^\circ$ were re-collected (data set 2). When the temperature was subsequently raised to 291 K rather quickly (within seconds), the crystal cracked and could not be used for further measurements.

Data processing. The intensities of the data set were scaled according to the two monotonously decreasing standards. The agreement between the two samples of symmetry-equivalent reflections is 0.021 [$R_1 = \Sigma \Delta v(I - \Delta v(I)) / \Sigma \Delta v(I)$] which

was considered reasonably satisfactory. Each number of counts, N was assigned a standard deviation of $\sigma(N) = [N + (0.005N)^2]^{1/2}$. Corrections for Lorentz and polarization effects, as well as for absorption (spherical crystal)¹¹ were applied to the net intensities. All calculations were performed on a Data General Eclipse S/230 computer, using programs designed by one of us (H. H.). After a preliminary refinement using the original full data set, an isotropic extinction correction was included, substituting the original values of F_o by $F_{\text{corr}} = F_o (1 + \alpha I_o)^{1/2}$. The parameter α was adjusted after further refinement to 1.06×10^{-6} . This increased F_o for the strongest reflections by approximately 70%, about 50 reflections being affected by more than 10%. Due to this rather severe extinction, the 90 strongest low-order reflections ($2\theta < 36^\circ$) were substituted from data set 2. An $(F_o/F_{\text{corr}})^2$ v.s. I_o plot indicated only negligible extinction in this data set. Furthermore, a correction for scan truncation errors was deemed necessary; Denne's method¹² was used, as in a number of previous cases.^{9,10,13,14}

Results and discussion

Least-squares refinements. Starting parameters were obtained from the previous room temperature study.⁶ Full-matrix least-squares refinements of atomic coordinates and thermal parameters were performed using the full data set (refinement I) as well as high-angle data only. In the high-angle refinements, various $\sin\theta/\lambda$ ranges were used. Varying $(\sin\theta/\lambda)_{\text{min}}$ and $(\sin\theta/\lambda)_{\text{max}}$ from 0.6 to 0.85 \AA^{-1} and 1.15 to 1.25 \AA^{-1} , respectively, caused no significant changes in coordinates and thermal parameters. The refinement with data in the range $0.80 < \sin\theta/\lambda < 1.25 \text{\AA}^{-1}$ (re-

Table 2. Refinement results.

	Refinement				
	I	II	III	IV	V
$\sin\theta/\lambda$ range/ \AA^{-1}	0.00–1.39	0.60–1.15	0.80–1.25	0.85–1.39	1.10–1.39
N_{obs}	4816	2649	2233	2689	1975
N_{var}	115	115	79	79	79
R^a	0.0222	0.0188	0.0186	0.0222	0.0239
S^b	1.90	1.21	1.08	1.27	1.29

$$^a R = \Sigma ||F_o| - |F_c|| / \Sigma |F_o|; \quad ^b S = [\Sigma w(|F_o| - |F_c|)^2 / (N_{\text{obs}} - N_{\text{var}})]^{1/2}.$$

Table 3. Fractional coordinates and thermal parameters, given by $\exp[-1/4(B_{11}h^2a^{*2} + \dots + 2B_{23}klb^*c^*)]$, for

Atom	Ref ^a	x	y	z	B_{11}
Cu	I	0	0	0	0.408(1)
	III	0	0	0	0.398(2)
	IV	0	0	0	0.415(2)
	V	0	0	0	0.429(2)
O1	I	0.26812(8)	0.07509(2)	0.00516(5)	0.540(8)
	III	0.26803(9)	0.07516(2)	0.00517(8)	0.536(7)
	IV	0.26796(9)	0.07517(3)	0.00524(9)	0.549(7)
	V	0.26792(12)	0.07519(3)	0.00522(14)	0.565(8)
O2	I	0.38499(10)	0.18830(3)	0.02642(5)	0.700(12)
	III	0.38487(12)	0.18827(3)	0.02632(7)	0.701(11)
	IV	0.38486(14)	0.18826(4)	0.02634(8)	0.716(10)
	V	0.38481(17)	0.18823(5)	0.02638(10)	0.731(12)
O3	I	-0.08499(9)	0.09898(3)	0.20066(4)	0.701(11)
	III	-0.08516(10)	0.09897(3)	0.20035(4)	0.640(10)
	IV	-0.08511(12)	0.09892(3)	0.20032(5)	0.666(9)
	V	-0.08502(15)	0.09892(4)	0.20033(6)	0.679(10)
O4	I	0.28624(10)	-0.06412(3)	0.14766(5)	0.776(12)
	III	0.28656(12)	-0.06425(3)	0.14751(6)	0.774(11)
	IV	0.28651(14)	-0.06427(4)	0.14743(6)	0.796(11)
	V	0.28644(17)	-0.06428(5)	0.14742(8)	0.805(13)
O5	I	0.41406(11)	0.30070(3)	0.18863(5)	0.916(14)
	III	0.41450(13)	0.30059(3)	0.18849(6)	0.916(12)
	IV	0.41462(16)	0.30056(4)	0.18849(7)	0.939(13)
	V	0.41474(21)	0.30051(5)	0.18850(9)	0.952(15)
N	I	-0.19871(10)	0.03929(3)	0.13888(5)	0.521(11)
	III	-0.19895(11)	0.03937(3)	0.13917(5)	0.513(9)
	IV	-0.19898(11)	0.03938(3)	0.13915(5)	0.524(9)
	V	-0.19892(14)	0.03932(4)	0.13913(7)	0.530(10)
C1	I	0.23065(11)	0.13906(3)	0.04525(5)	0.484(12)
	III	0.23066(11)	0.13896(3)	0.04516(6)	0.468(10)
	IV	0.23078(12)	0.13896(4)	0.04514(6)	0.480(10)
	V	0.23078(15)	0.13895(5)	0.04513(8)	0.493(11)
C2	I	-0.01556(13)	0.15396(3)	0.11684(6)	0.642(16)
	III	-0.01626(17)	0.15392(3)	0.11697(6)	0.586(16)
	IV	-0.01623(19)	0.15393(4)	0.11697(7)	0.589(19)
	V	-0.01611(25)	0.15390(5)	0.11693(10)	0.600(26)
H11	I	-0.202(2)	0.0079(5)	0.196(1)	1.07(22)
H12	I	-0.349(1)	0.0509(5)	0.116(1)	0.51(19)
H21	I	0.011(2)	0.1966(5)	0.169(1)	0.76(21)
H22	I	-0.160(1)	0.1610(5)	0.060(1)	0.70(19)
H41	I	0.224(3)	-0.1022(7)	0.162(1)	2.89(31)
H42	I	0.403(3)	-0.0722(7)	0.108(1)	2.76(30)
H51	I	0.410(2)	0.2703(7)	0.141(1)	2.45(28)
H52	I	0.557(3)	0.2994(6)	0.217(1)	1.96(27)

^aRefinement.

refinements I, III, IV and V.

B_{22}	B_{33}	B_{12}	B_{13}	B_{23}
0.387(2)	0.491(1)	-0.057(3)	0.107(3)	-0.109(3)
0.373(2)	0.462(2)	-0.047(3)	0.096(3)	-0.103(3)
0.397(2)	0.498(2)	-0.049(3)	0.100(3)	-0.099(3)
0.416(3)	0.514(3)	-0.046(5)	0.100(4)	-0.098(4)
0.478(9)	0.858(11)	-0.067(7)	0.147(11)	-0.149(10)
0.460(6)	0.843(12)	-0.058(6)	0.166(11)	-0.161(10)
0.479(7)	0.869(14)	-0.063(6)	0.151(11)	-0.135(11)
0.499(9)	0.884(19)	-0.061(7)	0.152(14)	-0.123(13)
0.568(11)	1.105(13)	-0.194(10)	0.151(11)	-0.045(10)
0.544(9)	1.106(11)	-0.204(8)	0.193(9)	-0.062(8)
0.576(10)	1.139(13)	-0.200(9)	0.188(10)	-0.069(10)
0.581(13)	1.162(16)	-0.199(11)	0.197(12)	-0.072(12)
0.657(11)	0.509(9)	-0.207(10)	0.022(9)	-0.114(8)
0.692(9)	0.480(8)	-0.174(8)	0.022(7)	-0.117(7)
0.712(11)	0.513(8)	-0.167(9)	0.030(7)	-0.116(7)
0.725(13)	0.526(9)	-0.152(10)	0.034(8)	-0.124(9)
0.629(12)	0.842(12)	0.010(10)	0.096(11)	0.006(10)
0.627(9)	0.793(11)	0.011(8)	0.071(9)	-0.011(8)
0.645(11)	0.814(11)	0.014(10)	0.078(9)	0.006(9)
0.652(14)	0.839(13)	0.019(12)	0.078(11)	0.013(10)
0.705(13)	0.901(13)	0.031(11)	-0.086(12)	-0.056(11)
0.683(10)	0.848(11)	0.036(9)	-0.077(10)	-0.039(9)
0.716(12)	0.901(12)	0.034(11)	-0.068(11)	-0.034(10)
0.726(15)	0.925(15)	0.031(13)	-0.068(13)	-0.033(12)
0.511(12)	0.572(11)	-0.062(10)	0.033(9)	-0.082(9)
0.533(9)	0.536(9)	-0.034(8)	0.059(8)	-0.074(7)
0.557(11)	0.557(9)	-0.039(8)	0.052(7)	-0.073(8)
0.578(13)	0.576(10)	-0.039(10)	0.050(8)	-0.074(9)
0.494(13)	0.594(13)	-0.028(11)	0.000(11)	-0.007(10)
0.442(9)	0.613(10)	-0.044(8)	0.023(9)	-0.029(8)
0.476(11)	0.634(11)	-0.042(9)	0.035(9)	-0.014(9)
0.481(14)	0.649(13)	-0.040(11)	0.034(10)	-0.026(11)
0.510(12)	0.819(13)	-0.008(13)	0.128(13)	-0.070(10)
0.501(9)	0.798(11)	-0.004(11)	0.128(12)	-0.098(8)
0.530(10)	0.828(12)	0.009(11)	0.123(12)	-0.084(9)
0.550(13)	0.841(14)	0.006(14)	0.121(14)	-0.072(11)

Table 4. Bond distances (Å) and angles (°) for non-hydrogen atoms obtained from refinements I, III and IV, and from the room temperature study.

Atoms	I	III	IV	Room temp. ^a
Cu—O1	1.9755(4)	1.9761(4)	1.9760(5)	1.967(1)
Cu—O4	2.5007(5)	2.5018(6)	2.5013(7)	2.545(1)
Cu—N	1.9790(5)	1.9826(6)	1.9826(6)	1.978(1)
O1—C1	1.2927(7)	1.2893(7)	1.2886(10)	1.286(1)
O2—C1	1.2371(8)	1.2378(8)	1.2371(10)	1.234(1)
C1—C2	1.5197(9)	1.5243(10)	1.5248(11)	1.516(1)
C2—O3	1.4275(7)	1.4233(8)	1.4239(10)	1.423(1)
O3—N	1.4345(7)	1.4302(8)	1.4295(8)	1.435(1)
O1—Cu—N	94.32(2)	94.28(3)	94.26(3)	94.28(3)
O1—Cu—O4	84.87(2)	84.91(2)	84.92(3)	84.65(3)
N—Cu—O4	89.23(2)	89.29(2)	89.31(2)	89.12(3)
Cu—O1—C1	124.54(4)	124.57(4)	124.64(4)	124.86(5)
O1—C1—O2	122.69(5)	122.74(6)	122.81(7)	122.72(7)
O1—C1—C2	118.14(5)	118.16(5)	118.11(6)	118.26(7)
O2—C1—C2	119.16(5)	119.09(5)	119.07(7)	119.02(7)
C1—C2—O3	114.20(5)	114.06(5)	114.02(7)	114.28(8)
C2—O3—N	111.25(4)	111.54(5)	111.56(5)	111.11(8)
O3—N—Cu	116.26(4)	116.10(4)	116.08(4)	116.19(6)

^aRef. 6.

finement III) gave the best goodness-of-fit parameter ($S = 1.08$) and the lowest R -values ($R = 0.0186$, $R_w = 0.0197$). When data with $\sin\theta/\lambda > 1.25 \text{ \AA}^{-1}$ are included in the refinement, S increases, and the thermal parameters are significantly changed as compared to the high-angle refinements with $(\sin\theta/\lambda)_{\max} \leq 1.25 \text{ \AA}^{-1}$. The thermal parameters increase, indicating underestimation of the truncation correction,¹⁴ and/or a scale factor difference. However, other factors also

seem to be involved, since the B_{11} , B_{22} and B_{33} values are affected differently for the various atoms (see Table 3 and compare results of refinements IV and V with those of refinement III). Whether this anisotropic effect is caused by anharmonicity of thermal vibrations, or contains information on the aspherical electron distribution, or is an artefact due to errors in the high-angle data measurements, is not clear. The selection of symmetry-related reflections collected did

Table 5. Bond distances (Å) and angles (°) involving hydrogen atoms, from the full-angle refinement I.

Distance		Distance	
C2—H21	0.99(1)	C2—H22	0.98(1)
N—H11	0.86(1)	N—H12	0.84(1)
O4—H41	0.80(1)	O4—H42	0.76(1)
O5—H51	0.78(1)	O5—H52	0.80(1)
Angle		Angle	
C1—C2—H21	109.4(6)	C1—C2—H22	109.6(6)
O3—C2—H21	104.1(6)	O3—C2—H22	109.1(6)
H21—C2—H22	110.3(9)	H11—N—H12	111.9(1.0)
Cu—N—H11	108.4(8)	Cu—N—H12	110.5(7)
O3—N—H11	101.4(8)	O3—N—H12	108.2(7)
Cu—O4—H41	108.4(1.0)	Cu—O4—H42	101.1(1.1)
H41—O4—H42	104.6(1.4)	H51—O5—H52	105.4(1.3)

not indicate larger discrepancy in the high-order region, although the sample may have been too small to reveal the problem. Without more extensive data we do not find it justified to attempt a chemical interpretation of the observed changes.

Hydrogen parameters were refined with isotropic temperature factors with the full data set, and in some refinements with data in the $\sin\theta/\lambda$ range 0.60–1.25 \AA^{-1} . Previous investigations have demonstrated the successful determination of hydrogen positions in light-atom structures by high-angle refinements.^{9,15} In the refinement of the present heavy atom structure, a refinement with $0.60 < \sin\theta/\lambda < 1.15 \text{\AA}^{-1}$ gave C–H bond lengths of 1.10(5) and 1.14(4) \AA , while the low cut-off had to be raised to $\sin\theta/\lambda = 0.70 \text{\AA}^{-1}$ to yield reasonable N–H distances, viz. 1.00(4) and 1.06(8) \AA ($0.70 < \sin\theta/\lambda > 1.25 \text{\AA}^{-1}$), in good agreement with results from light-atom structures. The O–H distances remained too short even at this cut-off, and the increased standard deviations in hydrogen positional parameters did not warrant further refinements. In all refinements with $(\sin\theta/\lambda)_{\min} > 0.70 \text{\AA}^{-1}$, hydrogen atoms were kept fixed at idealized bond distances (C–H = 1.09 \AA , N–H = 1.03 \AA , O–H = 0.98 \AA) and with bond angles as obtained from the full angle refinement. Further tests will have to be made to establish whether hydrogen positions can be adequately determined from high-angle refinements in heavy-atom structures.

The function minimized in all refinements was $\sum w(F_o - K|F_c|)^2$ where $w = 1/\sigma^2(F_o)$ and only data with $|F_o| > 3\sigma(F_o)$ were used. For non-hydrogen atoms, neutral atom scattering factors¹⁶ corrected for anomalous dispersion¹⁷ were used, and for hydrogen atoms, contracted spherical scattering factors.¹⁸ A summary of selected refinement results is given in Table 2, atomic parameters in Table 3, and bond distances and angles in Tables 4 and 5. Lists of structure factors may be obtained from one of the authors (J.S.) on request.

Comparison of the various refinement results shows that the atomic positions do not change significantly when $\sin\theta/\lambda$ is varied within $0.6 < \sin\theta/\lambda < 1.39 \text{\AA}^{-1}$ (see coordinates and bond distances and angles from refinements III and IV). The irregularity in thermal parameters observed when data with $\sin\theta/\lambda > 1.25 \text{\AA}^{-1}$ are included is not reflected in positional parameters. When low-angle data are included (refinement I) some of the positional parameters are, as ex-

pected, significantly affected. N and O3 are slightly displaced toward their lone-pairs, and C2 and C1 towards each other, resulting in longer O3–N and O3–C2 bonds, and shorter Cu–N and C2–C1 bonds, as well as small, but significant changes in bond angles at N and O3 (Fig. 1, Table 4). Comparison with the room-temperature low-angle refinement shows generally good agreement between the two structure determinations. The large deviation in the Cu–O4 distances probably arises because this weak bond is easily compressed as the cell volume decreases at lower temperatures.

Deformation density maps. Deformation effects become progressively smaller with increasing $\sin\theta/\lambda$. The best estimates of nuclear positions and atomic thermal parameters are accordingly to be expected from very high-angle refinement. In our case, refinements including data with $\sin\theta/\lambda > 1.25 \text{\AA}^{-1}$ had caused unexpected changes in thermal parameters as compared to other refinements. Thus, it was decided to prepare deformation density maps based on parameters determined both from refinements III ($0.80 < \sin\theta/\lambda < 1.25 \text{\AA}^{-1}$) and IV ($0.85 < \sin\theta/\lambda < 1.39 \text{\AA}^{-1}$). In each case the deformation density $\Delta\rho$ was defined as $\rho_{\text{obs}} - \sum \rho_{\text{spherical atoms}}$. The deformation density maps presented in Figs. 2 and 3 are based on parameters from refinement III, and include data up to $\sin\theta/\lambda = 1.00 \text{\AA}^{-1}$ in the calculations of $\Delta\rho$. The scale factor for the calculated density was obtained by one cycle of refinement on full data, $\sin\theta/\lambda < 1.25 \text{\AA}^{-1}$, and with fixed atomic parameters from refinement III.

Deformation density in the vicinity of the Cu ion is depicted in Figs. 2a–e. Prominent features are holes showing electron deficiencies, as compared to the spherical atom model, in directions towards the closest ligands, O1 and N, at distances of 0.57 and 0.67 \AA from Cu, respectively (Figs. 2a,d,e). There is no corresponding hole close to Cu on the long Cu–O4 bond. Corresponding features have also been observed in other studies of Jahn-Teller distorted copper complexes.^{2,5} Furthermore, extended regions of excess electron density are found in directions not pointing towards the ligating atoms, peak maxima being situated 0.40–0.55 \AA from Cu and directed approximately into the faces of the elongated octahedron defined by the ligands. According to simple crystal field theory a Cu^{2+} ion with

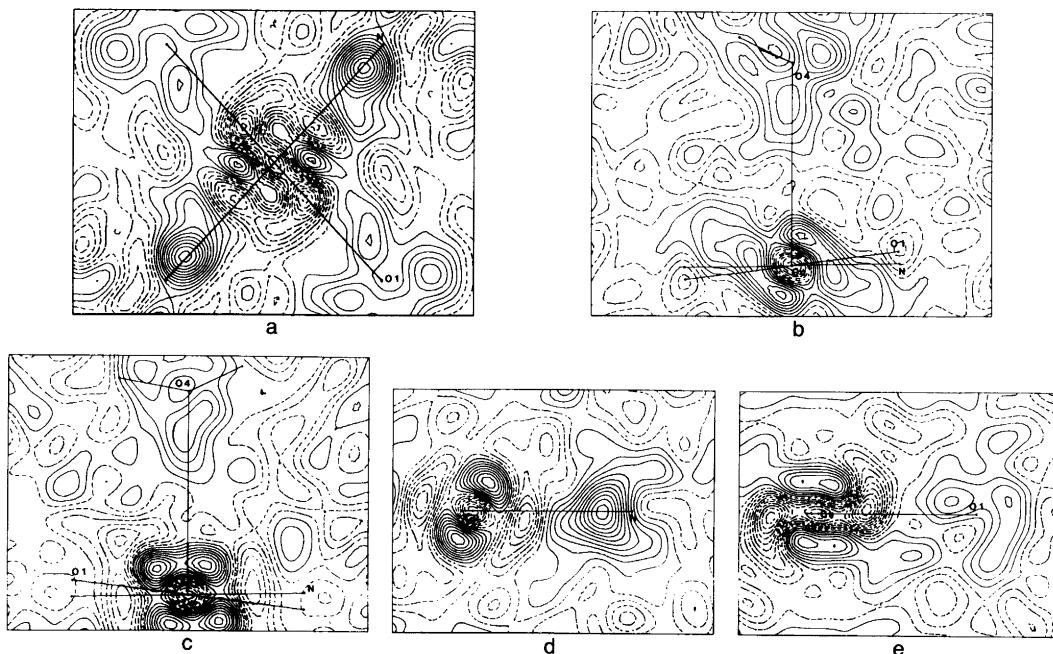


Fig. 2. Electron deformation density around Cu. Contour intervals are $0.07 \text{ e } \text{Å}^{-3}$; solid lines positive values, dashed lines zero and negative. (a) N-Cu-O1 plane; (b) plane through Cu-O4 and intersecting $\angle\text{N-Cu-O1}$; (O1 is pointing out of the paper plane); (c) plane through Cu-O4 and at 90° to the previous plane; (d) plane N-Cu-O4; (e) plane O1-Cu-O4.

elongated octahedral surroundings has orbital populations d_{xy}^2 , d_{xz}^2 , d_{yz}^2 , d_{z^2} , $d_{x^2-y^2}^2$. The electron deformation density observed is in qualitative agreement with such a picture. Results for other octahedral complexes have also been interpretable in terms of simple crystal field theory.¹⁹

To check how the features around Cu depend upon the selection of data included in the $\Delta\rho$ calculations, additional maps were calculated. When only structure factors up to $\sin\theta/\lambda = 0.8 \text{ Å}^{-1}$ are included, peak heights are slightly lower and troughs slightly shallower; otherwise the features remain unchanged. With only high-angle data in the range $0.8 < \sin\theta/\lambda < 1.25 \text{ Å}^{-1}$ included in the $\Delta\rho$ calculation, lone-pair and bonding features around light atoms virtually vanish, as expected, while there are still sharp features close to Cu, in accordance with the expectation that *d*-electron scattering extends far out in reciprocal space. The general picture of holes in the Cu-O1 and Cu-N regions, and peaks in directions between ligands is retained, while relative peak heights change appreciably. Departure from two-

fold symmetry around Cu-O4 in the electron density close to Cu, noticeable in Fig. 2, becomes more pronounced. In some previous cases asymmetry has been related to second-nearest-neighbour interaction.^{1,2} In the present case such a discussion is not warranted.

As shown in Fig. 2, the lone-pair density of N and O4 points directly towards Cu, while O1 lone-pair density is slightly displaced from the Cu-O1 bond. In Fig. 3, deformation densities in lone pairs and bonding regions of the remaining light atoms are depicted. Peak heights and positions are generally consistent with findings in light-atom structures.^{13,20} A notable feature is the lack of deformation density in the N-O bond. This is in agreement with findings for, e.g., *p*-nitropyridine²¹ and *N*-phenyl-substituted sydnone.²² Surprisingly low densities have also been observed in N-N, O-O and C-F bonds.^{23,24} Low electron density in the bond region between electron-rich atoms thus seems to be a consistent feature in experimental electron density studies.²⁴

Deformation density maps based on the struc-

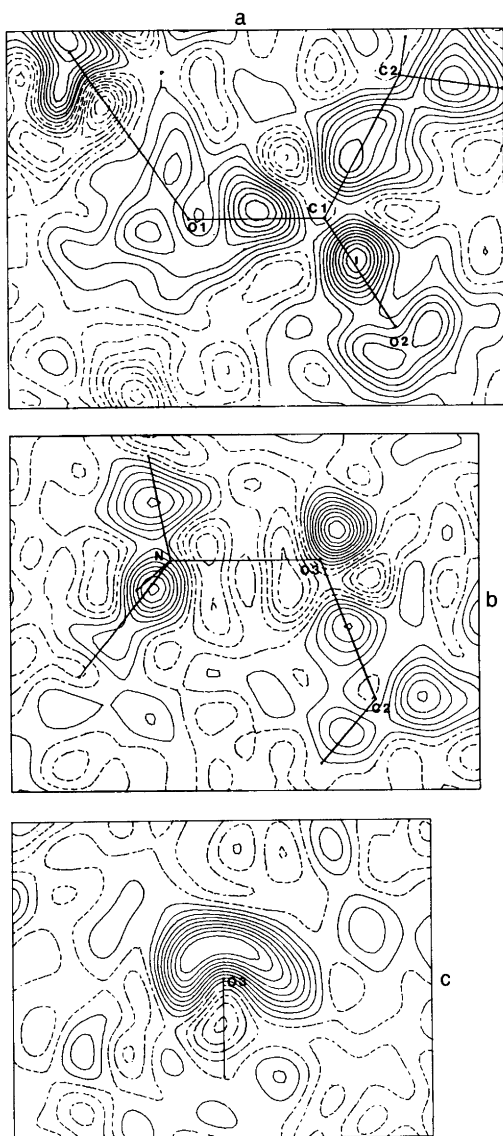


Fig. 3. Electron deformation density in the ligand; contour intervals as in Fig. 2. (a) Plane through O1-C1-O2. C2 is only 0.02 Å from this plane (the Cu-O1 bond is indicated although Cu lies 0.38 Å below the plane depicted); (b) N-O3-C2 plane (Cu lies 1.4 Å above this plane); (c) section through maximum of O3 lone-pair region and normal to plane in (b).

ture model from refinement IV ($0.85 < \sin\theta/\lambda < 1.39 \text{ \AA}^{-1}$ included in refinement) show only

minor changes near the light atoms, bond peaks being slightly more irregular than those presented in Fig. 3 (based on refinement III). In the vicinity of Cu there are more pronounced changes, the deviation from two-fold symmetry around Cu-O4 now becoming appreciable. Even so, the features indicating electron deficiency in directions towards the closest ligands, as well as excess electron density between ligands, remain.

Conclusions

High-angle refinements of data in shells of reciprocal space show changes in thermal parameters which might indicate anharmonicity. Electron deformation density maps based on atomic parameters from various shells show only small variations around the light atoms, while changes around Cu are appreciable. Despite these shortcomings, the general deformation density features around copper may qualitatively be interpreted in terms of simple crystal field theory. The data do not allow a more detailed evaluation of charge distribution and orbital population. For electron density studies of heavy-atom structures it seems important to collect enough symmetry related reflections to provide a solid basis for pinpointing systematic errors in the data.

References

1. Maslen, E. N., Spadaccini, N. and Watson, K. J. *Acta Crystallogr., Sect. B* 42 (1986) 430.
2. Varghese, J. N. and Maslen, E. N. *Acta Crystallogr., Sect. B* 41 (1985) 184.
3. Tanaka, K. and Marumo, F. *Acta Crystallogr., Sect. B* 38 (1982) 1422.
4. Figgis, B. N., Reynolds, P. A., White, A. H. and Williams, G. A. *J. Chem. Soc., Dalton Trans.* (1981) 371.
5. Tanaka, K., Konishi, M. and Marumo, F. *Acta Crystallogr., Sect. B* 35 (1979) 1303.
6. Sletten, J. *Acta Chem. Scand. Ser. A* 36 (1982) 583.
7. Zvilichovsky, G. *Tetrahedron* 22 (1966) 1445.
8. Harel, M. and Hirshfeld, F. L. *Acta Crystallogr., Sect. B* 31 (1975) 162.
9. Hope, H. and Ottersen, T. *Acta Crystallogr., Sect. B* 34 (1978) 3623.
10. Hirshfeld, F. L. and Hope, H. *Acta Crystallogr., Sect. B* 36 (1980) 406.
11. *International Tables for X-Ray Crystallography*, Kynoch Press, Birmingham 1962, Vol. II, pp. 302-305.

SLETTEN AND HOPE

12. Denne, W. A. *Acta Crystallogr., Sect. A* 33 (1977) 438.
13. Ottersen, T. and Hope, H. *Acta Crystallogr., Sect. B* 35 (1979) 373.
14. Eisenstein, M. *Acta Crystallogr., Sect. B* 35 (1979) 2614.
15. Hope, H. and Nichols, B. G. *Acta Crystallogr., Sect. A* 37 (1981) C136.
16. Cromer, D. T. and Mann, J. B. *Acta Crystallogr., Sect. A* 24 (1968) 321.
17. Cromer, D. T. and Liberman, D. *J. Chem. Phys.* 53 (1970) 1891.
18. Stewart, R. F., Davidson, E. R. and Simpson, W. T. *J. Chem. Phys.* 42 (1965) 3175.
19. Figgis, B. N., Reynolds, P. A. and Wright, S. *J. Am. Chem. Soc.* 105 (1983) 434 and references therein.
20. Coppens, P. *Acta Crystallogr., Sect. A* 40 (1984) 184.
21. Coppens, P. and Lehmann, M. S. *Acta Crystallogr., Sect. B* 32 (1976) 1777.
22. Hope, H. *Acta Crystallogr., Sect. A* 34 (1978) S20.
23. Hope, H. and Ottersen, T. *Acta Crystallogr., Sect. B* 35 (1979) 370 and references therein.
24. Dunitz, J. D. and Seiler, P. *J. Am. Chem. Soc.* 105 (1983) 7056 and references therein.

Received June 5, 1987.